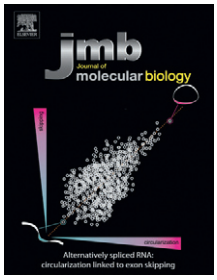

Anti-PolyQ Antibodies Recognize a Short PolyQ Stretch in Both Normal and Mutant Huntingtin Exon 1

Gwen E. Owens [1,2], Danielle M. New [1], Anthony P. West Jr. [1] and Pamela J. Bjorkman [1,3]

1 - Division of Biology and Biological Engineering, *California Institute of Technology, 1200 East California Boulevard, Pasadena, CA 91125, USA*
2 - Graduate Option in Biochemistry and Molecular Biophysics, *California Institute of Technology, 1200 East California Boulevard, Pasadena, CA 91125, USA*
3 - Howard Hughes Medical Institute, *4000 Jones Bridge Road, Chevy Chase, MD 20815-6789, USA*

Correspondence to Pamela J. Bjorkman: *1200 East California Boulevard, MC 114-96, Pasadena, CA 91125, USA.*
bjorkman@caltech.edu
http://dx.doi.org/10.1016/j.jmb.2015.05.023
Edited by S. Sidhu

Abstract

Huntington's disease is caused by expansion of a polyglutamine (polyQ) repeat in the huntingtin protein. A structural basis for the apparent transition between normal and disease-causing expanded polyQ repeats of huntingtin is unknown. The “linear lattice” model proposed random-coil structures for both normal and expanded polyQ in the preaggregation state. Consistent with this model, the affinity and stoichiometry of the anti-polyQ antibody MW1 increased with the number of glutamines. An opposing “structural toxic threshold” model proposed a conformational change above the pathogenic polyQ threshold resulting in a specific toxic conformation for expanded polyQ. Support for this model was provided by the anti-polyQ antibody 3B5H10, which was reported to specifically recognize a distinct pathologic conformation of soluble expanded polyQ. To distinguish between these models, we directly compared binding of MW1 and 3B5H10 to normal and expanded polyQ repeats within huntingtin exon 1 fusion proteins. We found similar binding characteristics for both antibodies. First, both antibodies bound to normal, as well as expanded, polyQ in huntingtin exon 1 fusion proteins. Second, an expanded polyQ tract contained multiple epitopes for fragments antigen-binding (Fabs) of both antibodies, demonstrating that 3B5H10 does not recognize a single epitope specific to expanded polyQ. Finally, small-angle X-ray scattering and dynamic light scattering revealed similar binding modes for MW1 and 3B5H10 Fab–huntingtin exon 1 complexes. Together, these results support the linear lattice model for polyQ binding proteins, suggesting that the hypothesized pathologic conformation of soluble expanded polyQ is not a valid target for drug design.

Introduction

Huntington's disease (HD) is a fatal neurodegenerative disorder characterized clinically by psychiatric symptoms, cognitive decline, and uncontrolled movements [1]. HD is caused by expansion of a CAG repeat within exon 1 of *HTT* (previously *HD*) that encodes an expanded polyglutamine (polyQ) tract in the N-terminal portion of the huntingtin protein. A pathologic threshold exists for HD, in which HD is fully penetrant in patients with 42 or more glutamines in the huntingtin protein, but no disease is found in individuals with 36 or fewer glutamines, while huntingtin with 37–41 glutamines exhibits reduced HD penetrance [2]. Although a structural basis for an apparent normaldisease threshold is unknown, several hypotheses exist for the conformation of monomeric, soluble polyQ in normal and expanded huntingtin protein.

The “linear lattice” hypothesis proposed that polyQ retains a random-coil structure for both normal and expanded polyQ in the preaggregation state. In this model, the increase in number of binding epitopes in expanded polyQ compared with normal polyQ

results in avidity effects that cause higher apparent affinities for bivalent proteins such as antibodies [3]. This could induce altered binding interactions with other cellular proteins or other polyQ repeats, leading to neuronal toxicity. Consistent with this model, the affinity of the anti-polyQ antibody MW1 to huntingtin amino-terminal protein encoded by exon 1 (hereafter called huntingtin exon 1 protein) increased in a polyQ-length-dependent manner, and binding of multiple fragments antigen-binding (Fabs) of MW1 to expanded polyQ tracts was observed. In addition, huntingtin exon 1 protein with 16–46 glutamines exhibited a random-coil conformation in solution, and no evidence was found for a global conformation change above 37 glutamines [3,4]. Surface plasmon resonance and analytical ultracentrifugation studies also demonstrated that multiple MW1 Fabs bound to expanded polyQ tracts [3]. The X-ray crystal structure of a $GQ_{10}G$ peptide bound to the variable regions of MW1 revealed that a short polyQ tract adopted an extended structure in a diagonal binding groove across the antigen-binding site of MW1 [4]. Additional binding studies using the anti-polyQ antibody 1C2 [5] showed that 1C2 also exhibited preferential binding to expanded polyQ due to avidity effects, and this preferential binding was not due to a mutant huntingtin-specific toxic structure recognized by 1C2 [6].

In contrast, the "structural toxic threshold" model proposed that a conformational transition occurs in polyQ repeats that are longer than the pathological threshold, which results in a specific toxic conformation for monomeric expanded polyQ that could potentially be recognized by antibodies [7]. According to this model, the postulated pathologic conformation could be directly toxic or it could alter interactions between mutant huntingtin and its binding partners; in either case, the pathologic conformation could be targeted for drug design. Support for this model was provided by studies of the anti-polyQ antibody 3B5H10, which was reported to recognize a single epitope representing a distinct pathologic conformation of soluble expanded polyQ [8,9]. In these studies, 3B5H10 IgG preferentially bound to expanded polyQ, and a two-stranded β-hairpin conformation of polyQ was modeled into the predicted polyQ-binding groove of the 3B5H10 Fab structure [9]. Support for this model was provided by a gel-filtration assay of 3B5H10 Fab binding to a Q_{39}-containing huntingtin exon 1 fusion (HD-39Q) protein, which was interpreted to demonstrate a 3B5H10 Fab:HD-39Q binding stoichiometry of 1:1 [8]. These results were suggested to indicate that 3B5H10 binds to a single structured polyQ epitope only present in expanded polyQ, as per the structural toxic threshold hypothesis. Modeling of small-angle X-ray scattering (SAXS) data was interpreted as showing that 3B5H10 Fab bound to HD-39Q in a 2:2 3B5H10 Fab:HD-39Q complex in which each 3B5H10 Fab recognized one subunit of an HD-39Q dimer through binding to a two-stranded β-hairpin conformation of polyQ [9]. Contradictory evidence was provided by a recent report demonstrating that pull-down assays and surface plasmon resonance studies showed that 3B5H10 IgG, like MW1 and 1C2 IgGs, could bind to short polyQ tracts, as expected given the high degree of sequence and structural similarities among the three antibodies [6].

Here we compared the recognition properties of the anti-polyQ monoclonal antibodies MW1 and 3B5H10 by studying their interactions with a polyQ-containing fragment of huntingtin. Using expressed and purified huntingtin exon 1-thioredoxin (TRX) fusion proteins containing 16–46 glutamines (HD-16Q, HD-25Q, HD-39Q, and HD-46Q) (Fig. 1a), we directly compared the interactions between soluble huntingtin and these anti-polyQ antibodies using biochemical and biophysical analysis techniques. We found that both MW1 and 3B5H10 antibodies exhibited similar binding properties, with neither providing evidence for a toxic conformation of expanded polyQ. These results argue against strategies designed to target a novel toxic conformation of soluble mutant huntingtin exon 1 protein in the preaggregation state.

Results

Both MW1 and 3B5H10 antibodies bind to normal and expanded polyQ within huntingtin exon 1 proteins

Western blots were used to evaluate the binding of 3B5H10 and MW1 IgGs to equimolar amounts of huntingtin exon 1-TRX fusion proteins and to the TRX tag alone (Fig. 1b). If 3B5H10 recognizes a toxic conformation present only in expanded polyQ, then it should not bind to short polyQ repeats unlike MW1. In contrast with some previous results [9] but consistent with other results [10,11], we found that both MW1 and 3B5H10 IgGs bound in a manner similar to huntingtin exon 1 fusion proteins, each capable of binding to huntingtin exon 1 proteins containing both normal and expanded polyQ repeats. Both IgGs bound to huntingtin exon 1 proteins in a polyQ-dependent manner, with a progressively more intense signal with increased polyQ length. Based on these results and previous Western blots demonstrating the ability of 3B5H10 to bind to glutathione *S*-transferase-polyQ with both short and long polyQ repeats [6], we conclude that both antibodies recognize a similar polyQ epitope that is present in both normal and expanded huntingtin exon 1 proteins.

In order to determine how it is possible to obtain results appearing to indicate that 3B5H10 binds only to expanded polyQ, we examined binding of 3B5H10 and MW1 as a function of concentration to huntingtin exon 1 proteins with different polyQ repeat lengths. Dot blots of serial dilutions of huntingtin exon 1

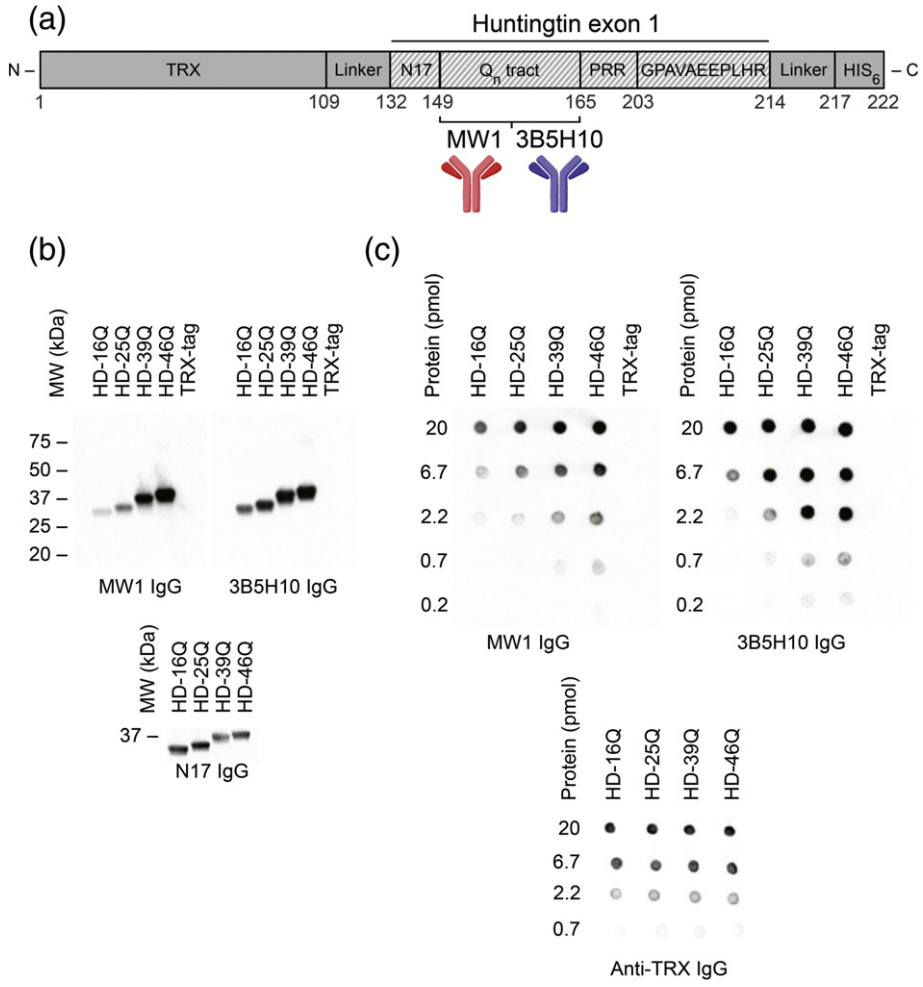

Fig. 1. Biochemical analyses of huntingtin exon 1:3B5H10 IgG and huntingtin exon 1:MW1 IgG complexes. (a) Schematic of organization of human huntingtin exon 1-TRX fusion proteins used in this study. The bar above the domain structure represents the huntingtin exon 1 fragment with the polyQ tract indicated by a bracket. N17, N-terminal 17-amino-acid domain. PRR, proline-rich region. (b) Western blot analysis of 3B5H10 and MW1 IgG binding to huntingtin exon 1 fusion proteins with variable numbers of glutamines. Both MW1 and 3B5H10 IgGs bound to huntingtin exon 1 proteins with normal and expanded polyQ repeats but did not bind the TRX tag control (top panels). Equimolar loading of huntingtin exon 1 fusion proteins was verified by blotting with the N17 antibody that recognizes the first 17 residues of huntingtin [30] (bottom panel). Densitometry of bands in blots is shown in Fig. S1b. (c) Dot blot analysis of 3B5H10 and MW1 IgG binding to huntingtin exon 1 fusion proteins (top panels). Equimolar loading of huntingtin proteins was verified by blotting with anti-TRX (bottom panel). Densitometry results are shown in Fig. S1c. As huntingtin concentrations decreased, binding to short polyQ repeats of huntingtin exon 1 protein was reduced more than binding to long polyQ repeats for both anti-polyQ antibodies MW1 and 3B5H10.

proteins demonstrated that both 3B5H10 and MW1 IgGs bound to huntingtin exon 1 proteins in a length- and concentration-dependent manner (Fig. 1c). At higher concentrations of huntingtin exon 1 protein, both IgGs recognized huntingtin exon 1 constructs with polyQ tracts ranging from Q_{16} to Q_{46}. However, at lower concentrations of huntingtin exon 1 protein, a more intense signal was observed for the huntingtin exon 1 construct with the longest polyQ repeat (HD-46Q) compared to the construct with the shortest polyQ repeat (HD-16Q) (Fig. S1b and c). Due to the length- and concentration-dependent binding, conditions can be found under which MW1 or 3B5H10 IgG appeared to only bind expanded polyQ, thus explaining previously reported results that 3B5H10 only recognizes huntingtin with expanded polyQ [9]. However, for both antibodies, the binding dependence on polyQ length was progressive, without a distinct threshold at polyQ lengths >37Q. Thus, avidity effects resulted in bivalent IgG

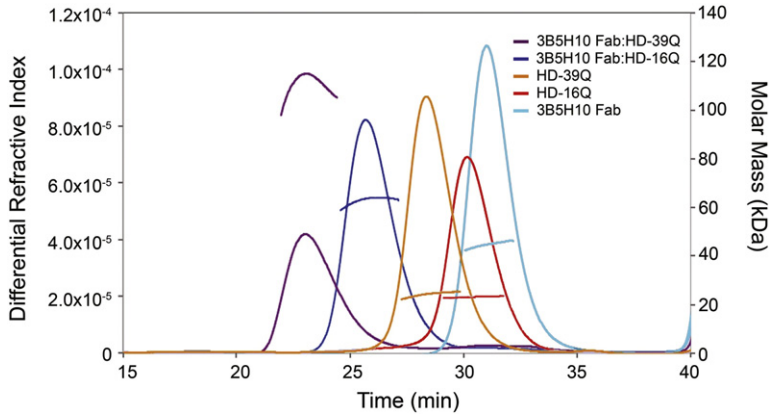

Fig. 2. SEC-MALS profiles of huntingtin exon 1 protein and Fab:huntingtin exon 1 complexes. Complexes were prepared with ~3-fold molar excess of Fab for experiments with HD-39Q and approximately equal molar ratios for experiments with HD-16Q and then injected onto a Superdex 200 10/300 GL gel-filtration column. The differential refractive index (left axis) is plotted against elution time from a gel-filtration column and overlaid with the molar mass determined for each peak (right axis).

versions of 3B5H10 and MW1 showing preferential binding to expanded polyQ, as predicted by the linear lattice model for antibody interactions with polyQ repeats [3,12].

Huntingtin exon 1 proteins are monomeric in solution

During purification of huntingtin exon 1 fusion proteins, we observed anomalous migration by gel-filtration chromatography such that huntingtin exon 1 fusion proteins appeared to migrate as higher-molecular-weight proteins (e.g., dimers) when compared with molecular weight standards of globular proteins. To determine the oligomeric state of the huntingtin exon 1 fusion proteins, we used a combination of size-exclusion chromatography (SEC) with inline multiangle light scattering (MALS), a technique that can be used to determine the absolute molecular mass of a protein or complex independent of shape and model [13]. To evaluate the methodology, we first analyzed 3B5H10 Fab alone, which migrated as a single monodisperse peak whose derived molecular mass closely matched the mass calculated from the amino acid sequence (Fig. 2 and Table 1). HD-16Q and HD-39Q fusion proteins also migrated as monodisperse peaks, and their calculated molecular masses corresponded to monomers in each case (Table 1). Thus, the anomalous migration of each huntingtin exon 1 protein in positions expected for a dimeric version of a globular protein of the same molecular mass results from slower migration due to an elongated structure rather than from dimerization. In particular, no evidence was found for dimer formation for HD-39Q as predicted in a previous study involving the modeling of SAXS data [9].

Non-equilibrium gel-filtration chromatography analyses yield inconsistent apparent binding stoichiometries

We next replicated published non-equilibrium gel-filtration chromatography experiments that were conducted to determine the stoichiometry of binding between 3B5H10 Fab and huntingtin exon 1 protein with an expanded polyQ repeat using the same proteins: 3B5H10 Fab and HD-39Q [8]. By varying the ratio of 3B5H10 Fab to HD-39Q, we determined the ratio where the least amount of excess Fab or excess HD-39Q was detected, the method previously used to report a 1:1 3B5H10:HD-39Q binding stoichiometry [8]. Similar to the published results, we found that unbound 3B5H10 Fab was present at ratios greater than 1:1 3B5H10 Fab:HD-39Q, that unbound HD-39Q was present at ratios less than 1:1, and that the ratio where the least amount excess of Fab or excess HD-39Q could be detected was 1:1 (Fig. 3a). As a control, we repeated the non-equilibrium gel-filtration stoichiometry experiment to evaluate the binding behavior of MW1 Fab and HD-39Q (Fig. 3b), which was previously shown to form a complex with a greater than 1:1 stoichiometry [3]. Under non-equilibrium conditions, the stoichiometry of MW1 Fab:HD-39Q appeared to be less than 1:1. Thus, it appeared that non-equilibrium gel filtration could not be reliably used to derive an accurate binding stoichiometry for an anti-polyQ Fab binding to huntingtin exon 1 fusion proteins with expanded polyQ.

Table 1. SEC-MALS analysis of huntingtin exon 1 proteins and 3B5H10 Fab:huntingtin exon 1 complexes

Molecule or complex	SEC-MALS molecular mass (kDa)	
	Observed	Calculated
HD-16Q	23.1	24.3
HD-39Q	24.3	27.2
3B5H10 Fab	44.7	48.1
HD-16Q + 3B5H10 Fab	63.0	72.4 (1:1)
HD-39Q + 3B5H10 Fab	110.3	75.3 (1:1) 123.5 (2:1) 171.5 (3:1)

The observed and calculated molecular masses of the proteins are listed.

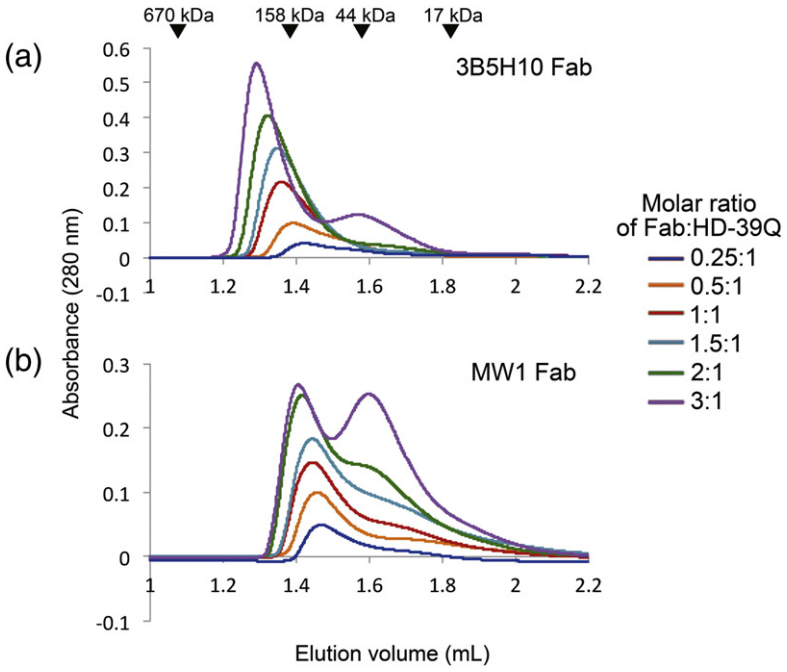

Fig. 3. Non-equilibrium gel-filtration chromatography analyses of Fab:HD-39Q complexes. Fabs of MW1 or 3B5H10 and HD-39Q were incubated at Fab:HD-39Q molar ratios of 0.25:1, 0.5:1, 1:1, 1.5:1, 2:1, and 3:1 and passed over a gel-filtration column run under non-equilibrium conditions. An HD-39Q concentration of 7 μM was used for all experiments. (a) 3B5H10 Fab in complex with HD-39Q. (b) MW1 Fab in complex with HD-39Q.

However, we noted that, with increasing molar ratios of 3B5H10 Fab:HD-39Q, the complex peak eluted earlier on the gel-filtration column, suggesting that a complex larger than 1:1 was forming at the same time as 3B5H10 Fab was dissociating from HD-39Q. Due to the anomalous migration of HD-39Q compared with globular proteins using gel-filtration chromatography (see above), the molecular mass of the 3B5H10 Fab:HD-39Q complex peak could not accurately be estimated based on gel-filtration migration. Using SEC-MALS, we found that the complex of 3B5H10 Fab and HD-39Q was polydisperse, and the molecular mass of the peak fraction corresponded to a complex composed of greater than a 1:1, but less than a 2:1, ratio of 3B5H10 Fab:HD-39Q (Table 1), demonstrating that dissociation of the complex occurred during the experiment. In contrast, the complex of 3B5H10 Fab and HD-16Q migrated as a monodisperse peak, and the calculated molecular mass for a 1:1 3B5H10 Fab:HD-16Q stoichiometric ratio was in close agreement with the molecular mass obtained by SEC-MALS (Table 1).

Taken together, the results for these experiments suggested that binding stoichiometries for MW1 and 3B5H10 Fabs binding to huntingtin exon 1 proteins as determined by non-equilibrium gel filtration are incorrect. This is likely because protein complexes that dissociate during this procedure are unable to rebind due to separation by the gel-filtration column. Therefore, depending on the binding kinetics and the amount of separation between anti-polyQ Fabs and huntingtin exon 1 proteins on the gel-filtration column, the binding stoichiometries determined by non-equilibrium gel-filtration techniques may be artificially low, as has been found in other protein–protein interaction systems evaluated by this technique [14,15].

Expanded polyQ tracts within huntingtin exon 1 proteins contain multiple epitopes for Fabs of MW1 and 3B5H10

To determine an accurate stoichiometry of binding between HD-39Q and the Fabs of 3B5H10 and MW1, we used equilibrium gel-filtration [16]. In this technique, a chromatography column is run with an equilibration buffer containing one of the binding partners (e.g., protein A). Different ratios of the binding partners (e.g., protein A and protein B) are then injected onto the column. When the amount of additional protein A injected is less than that required for formation of a complex, a trough will form at the position that protein A migrates. If the amount of additional protein A injected is in excess for complex formation, a peak is observed at the position that protein A migrates. When the amount of additional protein A injected is at the amount required for complex formation, a flat baseline is observed at the position that protein A migrates. However, unless the protein concentration in the equilibration buffer is much greater than the affinity of the protein–protein complex, the ratio of protein A to protein B at which a flat baseline is observed will not be an integer, in which case the correct stoichiometry can be obtained by rounding up to the next integer [14] or by

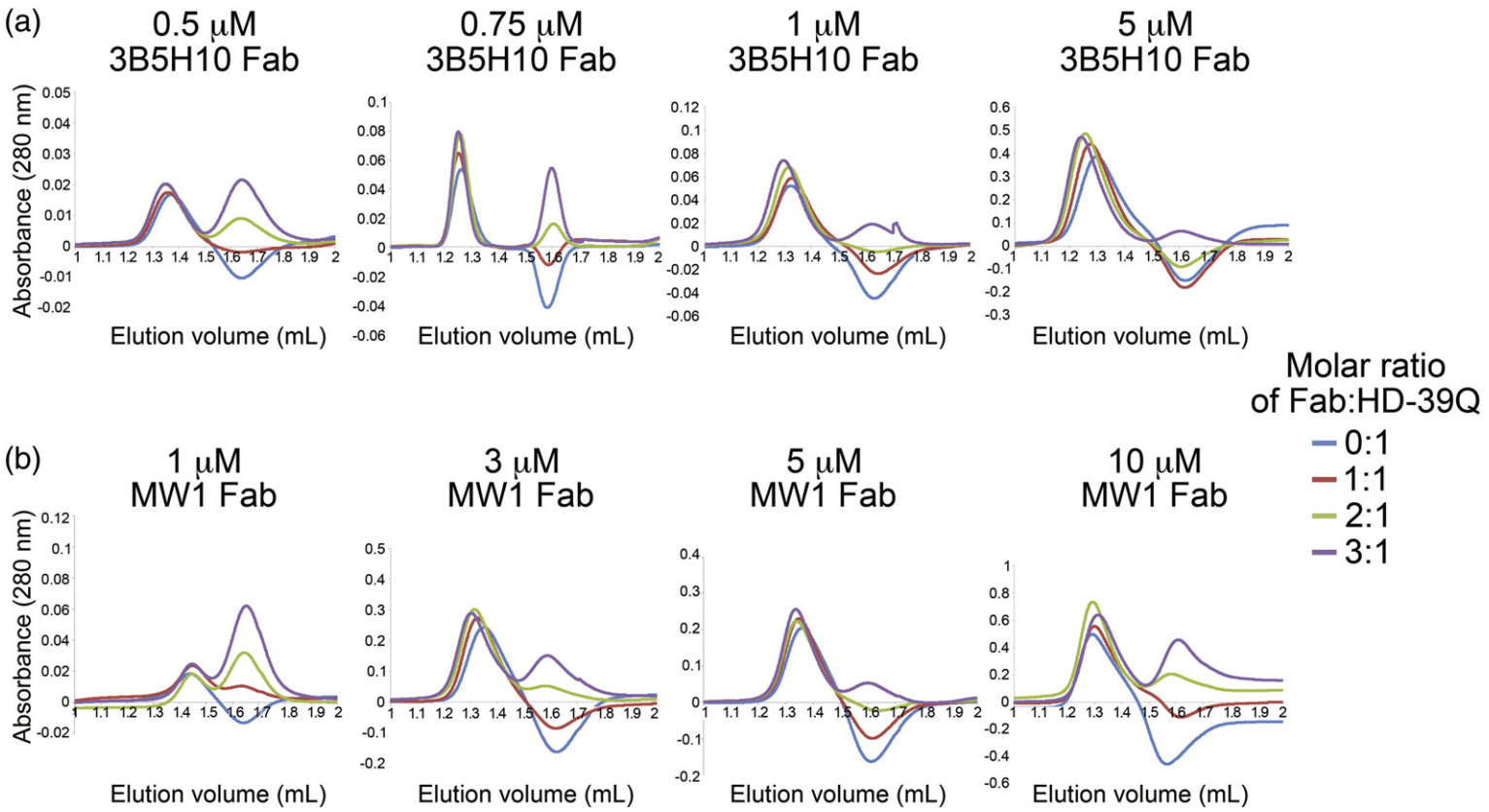

Fig. 4. Equilibrium gel-filtration chromatography analyses of Fab:HD-39Q complexes. MW1 or 3B5H10 Fabs and HD-39Q were incubated at the indicated molar ratios and passed over a gel-filtration column run in an equilibration buffer containing the indicated concentrations of 3B5H10 or MW1 Fab. For each experiment, HD-39Q at the same concentration as the Fab in the equilibration buffer was incubated with Fab at Fab:HD-39Q molar ratios of 0:1, 1:1, 2:1, and 3:1 in the equilibration buffer and injected onto a column that had been equilibrated in the equilibration buffer. The peak eluting first corresponds to a Fab:HD-39Q complex. The second peak or trough occurs at the volume where free Fab elutes. (a) 3B5H10 Fab in complex with HD-39Q using 0.5 μM, 0.75 μM, 1 μM, and 5 μM 3B5H10 Fab in the equilibration buffer. (b) MW1 Fab in complex with HD-39Q using 1 μM, 3 μM, 5 μM, and 10 μM MW1 Fab in the equilibration buffer. The Fab:HD-39Q stoichiometry approached 3:1 for both Fabs.

Table 2. Structural parameters of huntingtin exon 1 proteins, MW1 and 3B5H10 Fabs, and Fab:huntingtin exon 1 protein complexes from SAXS and DLS

Molecule or complex	MW (kDa), calculated	MW (kDa), observed	R_h (Å)	R_g (Å)	D_{max} (Å)	Porod volume (10^5) (Å^3)
3B5H10 Fab	48,118	54,900	33	28	98	0.6
MW1 Fab	47,330	49,300	33	26	87	0.6
HD-16Q	24,279	40,000	40	49	168	0.8
HD-39Q	27,226	21,700	47	52	164	0.9
3B5H10 Fab:HD-16Q	72,379	62,600	37	35	128	0.8
MW1 Fab:HD-16Q	71,609	71,200	41	40	141	0.9
3B5H10 Fab:HD-39Q	75,344 (1:1) 171,579 (3:1)	137,000–178,000	59	54	194	3
MW1 Fab:HD-39Q	74,556 (1:1) 169,216 (3:1)	125,000–162,000	52	50	173	2

Molecular weight (MW) observed, R_g, D_{max}, and Porod volume were obtained from SAXS. R_h was obtained from DLS. The extinction coefficient and theoretical molecular weight for a 3:1 and a 1:1 Fab:huntingtin exon 1 protein complex are different; therefore, a range of molecular weights are listed as observed for Fab:HD-39Q complexes. DLS and SAXS experiments were performed on the same samples. R_h, hydrodynamic radius. R_g, radius of gyration. D_{max}, the maximum linear dimension of scattered particles.

Scatchard analysis [15]. Previous measurements demonstrated a higher polyQ binding affinity for 3B5H10 Fab than for MW1 Fab: K_D = 1.0 μM for 3B5H10 Fab binding to a Q_{22} or Q_{41} peptide [6] *versus* K_D = 2.2 μM for MW1 Fab binding to HD-39Q [3]. Therefore, we used higher concentrations of MW1 Fab (1–10 μM) than 3B5H10 Fab (0.5–5 μM) in these experiments.

Complexes containing different ratios of Fab and HD-39Q were incubated together and injected onto a gel-filtration column equilibrated with the appropriate Fab. A series of experiments with different concentrations of 3B5H10 Fab in the equilibration buffer were performed. For example, for 5 μM 3B5H10 Fab in the equilibration buffer, the stoichiometry at which no peak or trough was observed was ~2.6:1 (Fig. 4a). Analysis with MW1 Fab yielded similar results, with the MW1 Fab:HD-39Q stoichiometry approaching 3:1 (Fig. 4b). Therefore, for both antibodies, the Fab:HD-39Q stoichiometry of binding was determined as 3:1.

Dynamic light scattering revealed similar sizes for complexes of MW1 and 3B5H10 Fabs with huntingtin exon 1 proteins

To further investigate complexes of anti-polyQ Fabs bound to huntingtin exon 1 proteins, we used dynamic light scattering (DLS) to compare hydrodynamic radii (R_h) of 3B5H10 and MW1 Fabs alone, HD-16Q and HD-39Q alone, and complexes of Fab and huntingtin exon 1 protein. Fab complexes with HD-16Q were prepared at a 1:1 Fab:HD-16Q molar ratio, while complexes with HD-39Q were prepared at a 3:1 molar ratio. Concentrations of proteins and complexes varied from 1 to 7 mg/mL, higher than the concentrations used for equilibrium gel-filtration experiments. As expected, the R_h values derived for the 3B5H10 and MW1 Fabs, which are globular proteins of similar dimensions, were roughly the same, and both R_h values were smaller than the R_h values for HD-16Q and HD-39Q (Table 2), consistent with the proposed elongated structures of HD-16Q and HD-39Q [3] (Table 2). Notably, the R_h value for HD-16Q was smaller than for HD-39Q, inconsistent with the compact structure proposed for expanded polyQ [9]. When complexed with huntingtin exon 1 proteins, both Fabs exhibited qualitatively similar behavior: the R_h values were lower for the Fab complexes with HD-16Q than with HD-39Q. Based on our gel-filtration and SEC-MALS data (Figs. 2 and 4), the complexes being examined by DLS were likely to be 1:1 Fab:HD-16Q complexes and a mixture of 2:1 and 3:1 Fab:HD-39Q complexes for both Fabs. Consistent with our other results, the 3B5H10 and MW1 Fabs did not exhibit different properties when binding to huntingtin exon 1 proteins as would have been expected if 3B5H10, but not MW1, recognized a pathologic conformation of expanded polyQ.

SAXS revealed similar predicted characteristics for complexes of MW1 and 3B5H10 Fabs with huntingtin exon 1 proteins

We next repeated published SAXS studies for HD-39Q alone and complexed with 3B5H10 Fab [9], comparing results with SAXS data for analogous complexes with MW1 Fab and HD-16Q. We collected SAXS data for samples of 3B5H10 and MW1 Fabs alone; HD-16Q, HD-25Q, HD-39Q, and HD-46Q alone; and complexes of each Fab with HD-16Q and HD-39Q. With the exception of the HD-46Q alone sample, the scattering profiles for the Fabs, huntingtin exon 1 fusion proteins alone, and Fab:HD-16Q and Fab:HD-39Q complexes showed ideal sample quality characteristics (Fig. S2). Guinier

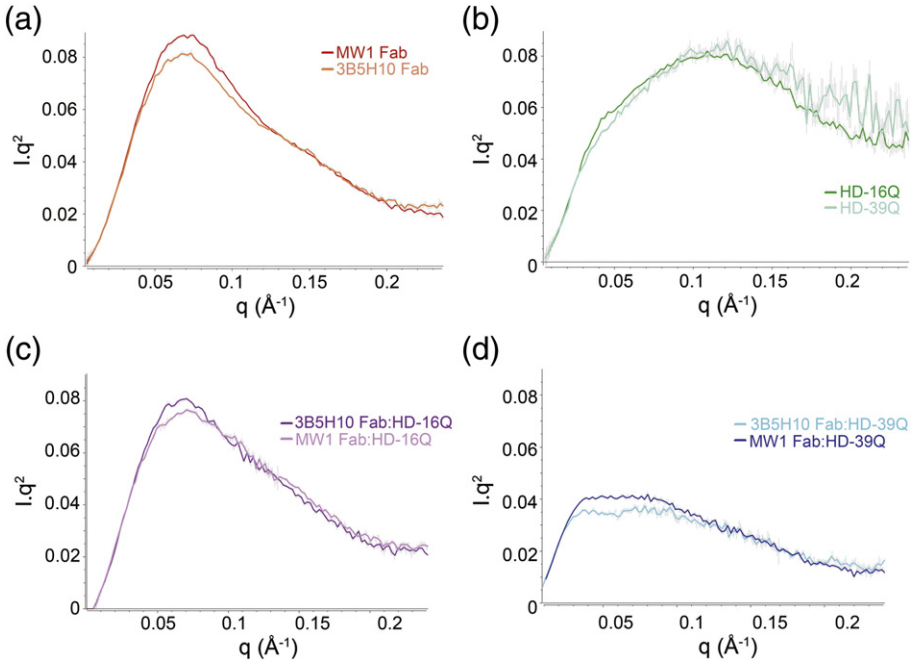

Fig. 5. Kratky plot analyses of SAXS data for huntingtin exon 1 fusion proteins, MW1 and 3B5H10 Fabs, and complexes of Fabs and huntingtin exon 1 proteins. Each plot shows the intensity of scattering plotted as Iq^2 *versus* q, where q is scattering angle ($Å^{-1}$) and I is the scattering intensity. (a) For MW1 and 3B5H10 Fabs, each plot exhibited one maximum, indicating that these are globular proteins. (b) HD-16Q and HD-39Q showed a plateau at higher q values, suggesting that these proteins include disordered regions, with decreasing globular character as the polyQ repeat length increased. (c) Curves for 3B5H10:HD-16Q and MW1:HD-16Q complexes were similar, each exhibiting broad single peaks. (d) Curves for 3B5H10:HD-39Q and MW1:HD-39Q complexes were similar, each exhibiting a similar low plateau.

analysis [17] indicated minimal aggregation for both Fabs alone and Fabs complexed with HD-16Q and HD-39Q and for all huntingtin exon 1 fusion proteins alone (Fig. S3). Radii of gyration (R_g) determined by SAXS were consistent with R_h values determined by DLS (Table 2). In particular, for measurements of huntingtin exon 1 fusion proteins alone, we did not see substantially increased R_h or R_g values for HD-39Q compared with HD-16Q, consistent with computational modeling of polyQ in aqueous solution suggesting that radii of polyQ tracts of increasing lengths are similar [18] but inconsistent with the structural toxic threshold model predicting a conformational transition for expanded polyQ tracts [9]. The predicted molecular weights of the complexes of 3B5H10 or MW1 Fab bound to HD-16Q in a 1:1 complex were similar to the molecular weights calculated based on the extrapolated scattering intensity at zero angle [19]. However, 3B5H10 Fab or MW1 Fab bound to HD-39Q formed complexes with observed molecular weights larger than a 1:1 complex. Based on molecular weight alone, these complexes could be 2:1, 3:1, or 2:2 Fab:HD-39Q complexes. A 2:2 3B5H10 Fab:HD-39Q stoichiometry was postulated to account for previous SAXS data [9]. However, our SEC-MALS and equilibrium gel-filtration data demonstrated that 3B5H10 Fab does not bind to HD-39Q in a 2:2 ratio (Fig. 2). Therefore, we interpret our SAXS data for both 3B5H10 and MW1 Fab binding to HD-39Q as evidence for mixtures of 2:1 and 3:1 Fab:HD-39Q complexes.

Kratky analysis was used to evaluate the relative degree of folding of each sample [20]. The Kratky plots for MW1 and 3B5H10 Fabs alone yielded bell-shaped peaks consistent with globular proteins [21,22] (Fig. 5a). By contrast, the Kratky plots for HD-16Q and HD-39Q were broader, with less decrease at higher scattering angles, consistent with flexible or unfolded proteins [21,22] (Fig. 5b). Thus, we found no evidence for a conformational change occurring for HD-39Q relative to HD-16Q. Similarly, we found no systematic differences for 3B5H10 *versus* MW1 Fab complexes with either HD-16Q or HD-39Q (Fig. 5c and d). These results are consistent with both Fabs exhibiting similar recognition properties for polyQ tracts.

Three-dimensional (3D) structures can be modeled into SAXS profiles; however, modeling is limited by the one-dimensional nature of SAXS data, and more than one 3D shape can produce the same one-dimensional scattering profile [23]. We did not attempt to fit atomistic models into the SAXS data as performed in a previous study [9] because (i) the complete 3D structure of huntingtin exon 1 protein is unknown, (ii) the polyQ tract within huntingtin exon 1

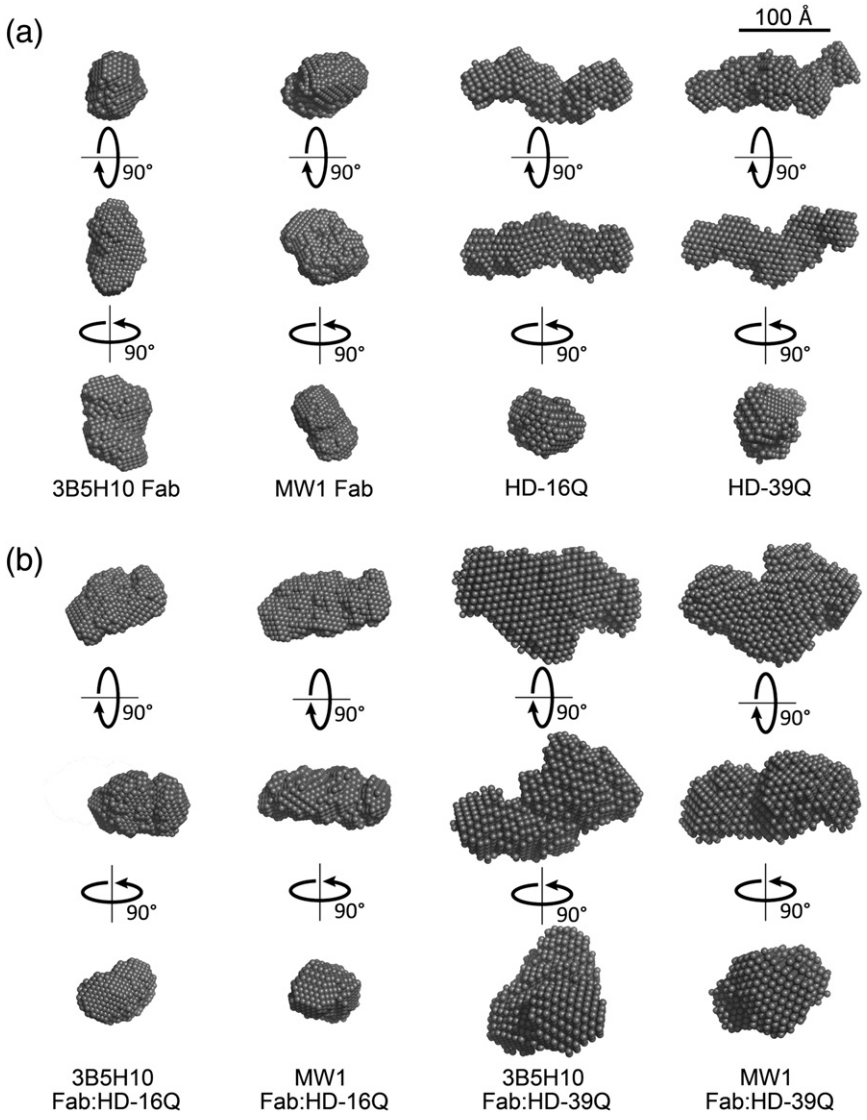

Fig. 6. *Ab initio* models derived from SAXS data for huntingtin exon 1 fusion proteins, MW1 and 3B5H10 Fabs, and Fab:huntingtin exon 1 complexes. Calculated molecular envelopes filled with dummy atoms reveal the shapes of (a) 3B5H10 Fab, MW1 Fab, HD-16Q, HD-39Q and (b) 3B5H10 Fab:HD-16Q, MW1 Fab:HD-16Q, 3B5H10 Fab:HD-39Q, MW1 Fab:HD-39Q.

fusion proteins adopts flexible random-coil structures in solution [3], and (iii) the arrangements among polyQ tracts, the remainder of huntingtin exon 1, the TRX fusion partner, and the His purification tag cannot be predicted. Nor did we assume that the huntingtin exon 1 fusion proteins were dimeric, as also performed for interpretation of SAXS data involving HD-39Q bound to 3B5H10 Fab [9], because our SEC-MALS data demonstrated that HD-39Q is monomeric in solution (Fig. 2). Instead, we used minimal assumptions to generate *ab initio* models that predicted molecular envelopes from the SAXS data for each of the well-behaved samples. We did not find notable differences between 3B5H10:HD-39Q and MW1:HD-39Q complexes based on R_g, D_{max}, or shape or volume of calculated envelopes (Fig. 6 and Table 2), as would be predicted by the toxic conformation model suggesting that 3B5H10, but not MW1, recognizes a compact conformation of expanded polyQ [9]. Instead, in agreement with experiments described above and in previous reports [3,4,6,12], the SAXS results were consistent with recognition of multiple epitopes within a linear lattice of expanded polyQ by both Fabs.

Discussion

The structure of huntingtin exon 1 protein in the preaggregation state, particularly the conformation

of the expanded polyQ repeat, is hypothesized to be critical in understanding the pathogenesis of HD. However, the structure of the basic components of huntingtin exon 1 remains controversial. An X-ray crystal structure of a Q_{17} huntingtin N-terminal region fused to MBP showed that a short polyQ region could adopt α-helical, loop, or random-coil conformations [24]. The structure of a Q_{10} peptide bound to the anti-polyQ antibody MW1 revealed an extended structure [4]. Other recent work suggested that the polyQ repeat acts as a flexible hinge that exhibits reduced flexibility at extended polyQ lengths [25]. In the present study, we show that the binding properties of the anti-polyQ antibodies MW1 and 3B5H10 support the "linear lattice" model for the structure of soluble polyQ in the context of a huntingtin exon 1 fusion protein. This model postulates that both normal and expanded polyQ tracts in the preaggregation state are random-coil structures, with expanded polyQ repeats containing more epitopes recognized by antibodies or other binding proteins than normal polyQ tracts [3]. Several lines of evidence, reported here and in previous publications [6,11], have shown that 3B5H10 and MW1 IgGs can bind to a normal polyQ repeat, demonstrating that neither antibody preferentially recognizes a novel structure formed by expanded polyQ but instead both recognize a short stretch of polyQ. This conclusion is in contrast to other studies suggesting that 3B5H10 bound preferentially to expanded polyQ repeats of mutant huntingtin according to a "structural toxic threshold" model, in which a conformational transition occurs in the polyQ repeat of huntingtin exon 1 protein at the pathologic threshold (>37Q) [9]. Instead, our results agree with the conclusions of a recent study comparing the binding of anti-polyQ antibodies 1C2 and 3B5H10 to polyQ repeats [6].

To evaluate whether an expanded polyQ tract contains one epitope for anti-polyQ Fabs as predicted by the structural toxic threshold model or multiple epitopes for the Fabs as predicted by the linear lattice model, we evaluated complexes using equilibrium gel-filtration chromatography. Our results demonstrated that the Fab:HD-39Q stoichiometry of both 3B5H10 Fab:HD-39Q and MW1 Fab:HD-39Q complexes was ~3:1 for both Fabs; thus, neither Fab preferentially recognizes a novel structure formed by expanded polyQ. Consistent with this result, we confirmed that both 3B5H10 and MW1 IgGs recognized unexpanded polyQ, in direct contradiction to the structural toxic threshold model. We also used SAXS and DLS to further study the conformation of normal and expanded forms of huntingtin exon 1 protein, alone and in complex with MW1 or 3B5H10 Fab. This allowed us to determine the globularity of the protein complexes and their approximate oligomeric states, which revealed striking similarities between MW1 and 3B5H10 Fabs, both when unliganded and when bound to HD-16Q or HD-39Q. Thus, a combination of equilibrium gel-filtration chromatography, DLS, and SAXS data are consistent with a linear lattice mode of recognition of unstructured polyQ for both 3B5H10 and MW1 antibodies. Sharing the same general ligand binding properties is consistent with the high degree of sequence and structural similarity relating 3B5H10 and MW1 [6]: the variable regions are related by 53% (V_H domain) and 99% (V_L domain) sequence identity and a root-mean-square deviation of 0.59 Å for superposition of V_H–V_L regions of the 3B5H10 (PDB code 3S96) and MW1 (PDB code 2GSG) crystal structures (calculated for all C^α atoms). In addition, the antigen-binding sites of both antibodies include an unusual diagonal groove [6] shown to accommodate a single extended stretch of polyQ in an MW1-polyQ co-crystal structure [4] and thus unlikely to bind to a two-stranded β-hairpin structure of polyQ, as modeled for the HD-39Q interaction with 3B5H10 Fab [9].

Reduced penetrance is seen in patients with between 37 and 41 glutamine repeats in the huntingtin protein, which may be best explained by a quantitative change in a rate-limiting process in which the effects can be countered in some patients and not in others due to environmental or genetic modifiers. This reduced penetrance is consistent with a continuous linear lattice effect that is weak at lower polyQ repeat lengths and progressively stronger at larger repeat lengths. These results are relevant to potential therapeutic approaches to target soluble expanded polyQ in a lag period preceding aggregation. As we find no evidence for recognition of a specific conformation of expanded polyQ within huntingtin exon 1 proteins in either this study or previous studies [3,4,6,12], we suggest that efforts to target expanded polyQ using monomeric binding partners are unlikely to be successful in discriminating polyQ stretches found in non-disease proteins such as transcription factors [26,27] from expanded polyQ within mutant huntingtin exon 1. Instead, we suggest strategies in which reagents that recognize short stretches of polyQ are covalently linked to allow avidity effects to discriminate between short and expanded polyQ tracts.

Materials and Methods

Protein expression and purification

Human huntingtin protein encoded by exon 1 (comprising 91 amino acids when containing 16 glutamine residues) including different-sized polyQ segments (Q16, Q25, Q39, and Q46) coded for by CAG or CAA/CAG repeats was expressed as a fusion protein with TRX. Exon 1 fusion proteins were purified as previously described [3] with the following modifications: autoinduction was used to culture cells to high densities [28], and sonication was used for cell lysis. Purified proteins were flash frozen and stored at −80 °C in 50 mM Tris (pH 8.0) and 150 mM NaCl.

MW1 IgG2b was purified from ascites fluid by protein A affinity chromatography (GE Healthcare). MW1 Fab was prepared by papain cleavage of MW1 IgG using a ratio of 1:25 (papain:MW1 by weight) for 30 min at 37 °C. Fabs were separated from the Fc fragment using protein A affinity chromatography (GE Healthcare) and then further purified by gel-filtration chromatography (Superdex 200 10/300 GL).

3B5H10 Fab was expressed and purified as previously described for other IgGs [29]. Briefly, the 3B5H10 light-chain gene and a C-terminally 6×-His-tagged heavy-chain gene were subcloned separately into the pTT5 mammalian expression vector (NRC Biotechnology Research Institute), and 3B5H10 Fab was expressed by transient co-transfection of HEK293-6E (NRC Biotechnology Research Institute) cells and purified from supernatants using Ni^{2+}-NTA affinity chromatography and gel-filtration chromatography (Superdex 200 10/300 or 16/60).

Protein concentrations were determined using 280 nm extinction coefficients of 80,830 M^{-1} cm^{-1} (3B5H10 Fab), 78,310 M^{-1} cm^{-1} (MW1 Fab), 14,180 M^{-1} cm^{-1} (TRX), 14,180 M^{-1} cm^{-1} (HD-16Q), and 14,180 M^{-1} cm^{-1} (HD-39Q). Extinction coefficients were calculated based on amino acid sequence using ProtParam[†].

Western and dot blot analyses

Equimolar amounts of purified huntingtin exon 1 protein and TRX were loaded and separated on an Any kD Mini-PROTEAN gel (Bio-Rad Laboratories, Hercules, CA) at 175 V for 40 min, followed by transfer to a nitrocellulose membrane at 100 V for 1 h. After blocking for 1 h in TBST with 3% bovine serum albumin, we incubated membranes overnight at 4 °C with 3B5H10 IgG (Sigma, St. Louis, MO), MW1 IgG (purified from ascites), or rabbit polyclonal N17 huntingtin IgG [30] at 1:75,000, 1:10,000 or 1:7500, respectively. Membranes were washed with TBST and incubated with HRP-conjugated anti-mouse IgG (Jackson Immunoresearch Laboratories, West Grove, PA) or HRP-conjugated anti-rabbit IgG (Jackson Immunoresearch Laboratories) for 1 h at room temperature. Membranes were washed again, and antibody binding was detected using Amersham Enhanced Chemiluminescence Prime Western Blotting Detection Reagent (GE Life Sciences, Uppsala, Sweden). Western blots were imaged using a ChemiDoc MP Imaging System (Bio-Rad Laboratories). Equimolar amounts of purified huntingtin exon 1 protein and TRX were also analyzed by SDS-PAGE on an Any kD Mini-PROTEAN gel (Bio-Rad Laboratories) and stained with Coomassie.

Equimolar amounts of huntingtin exon 1 fusion protein and TRX were serially diluted in 50 mM Tris (pH 8.0) and 150 mM NaCl and were spotted onto nitrocellulose membranes. Membranes were washed with TBST and probed with 3B5H10, MW1, or mouse monoclonal anti-TRX (Genscript, Piscataway, NJ) IgGs overnight at 4 °C. HRP-conjugated goat anti-mouse secondary antibody (Jackson Immunoresearch Laboratories) was used to quantitate antibody binding to proteins on the membrane, and antibody binding was detected using Amersham Enhanced Chemiluminescence Prime Western Blotting Detection Reagent (GE Life Sciences). Densitometry of blots was performed using Image Lab 5.2.1 Software (Bio-Rad Laboratories). Densities were expressed as a ratio relative to the density observed for HD-16Q (western blots) or 20 pmol HD-16Q (dot blots).

SEC-MALS

Purified proteins or protein complexes were characterized by SEC-MALS to determine absolute molecular masses [13]. Proteins were concentrated to 1 mg/mL, passed through a 0.2-μm filter (Millipore), and injected onto a Superdex 200 10/300 GL gel-filtration chromatography column equilibrated in a buffer containing 20 mM Tris (pH 8.0) and 100 mM NaCl. The chromatography system was connected with an 18-angle light-scattering detector (DAWN HELEOS II; Wyatt Technology), a dynamic light-scattering detector (DynaPro Nanostar; Wyatt Technology), and a refractive index detector (Optilab t-rEX; Wyatt Technology). Data were collected every second at a flow rate of 0.5 mL/min at 25 °C. Data analysis was carried out using the program ASTRA 6, yielding the molar mass and distribution of mass (polydispersity) of the sample.

Non-equilibrium gel-filtration chromatography

Non-equilibrium protein interaction experiments were carried out on a Superdex 200 PC 3.2/30 gel-filtration column (GE Healthcare) equilibrated in a buffer containing 50 mM Tris (pH 8.0) and 150 mM NaCl. A final concentration of 7 μM HD-39Q was used for all experiments, with 3B5H10 and MW1 Fab concentrations varied to create Fab:HD-39Q complexes with final molar ratios of 0.25:1, 0.5:1, 1:1, 1.5:1, 2:1, and 3:1. Of each complex, 50 μL was injected and flowed through the column at 50 μL/min at room temperature. The absorbance of the eluent was monitored at 280 nm.

Equilibrium gel-filtration chromatography

A Superdex 200 PC 3.2/30 (GE Healthcare) gel-filtration column was equilibrated and run with equilibration buffer: 50 mM Tris (pH 8.0), 150 mM NaCl, and a specific concentration of 3B5H10 Fab (0.5 μM, 0.75 μM, 1 μM, or 5 μM) or MW1 Fab (1 μM, 3 μM, 5 μM, or 10 μM). Complexes containing 0:1, 1:1, 2:1, or 3:1 molar ratios of a variable concentration of Fab:HD-39Q, where the concentration of HD-39Q was equal to the concentration of Fab in the equilibration buffer, were incubated for 30 min at room temperature in equilibration buffer and then injected onto the column. Chromatography was performed at a flow rate of 50 μL/min using a SMART micropurification system (Pharmacia), and the absorbance of the eluent was monitored at 280 nm.

Dynamic light scattering

DLS measurements were conducted on a DynaPro® NanoStar™ (Wyatt Technology, Goleta, CA) at 25 °C. All samples were purified using a Superdex 200 10/300 column in 50 mM Tris (pH 8.0) and 150 mM NaCl prior to DLS and SAXS measurements, and the same sample preparations were used for both experiments. Fractions were pooled and concentrated to at least 2 mg/mL and filtered through 0.2-μm membranes (Millipore). Samples

were equilibrated to 25 °C prior to DLS measurements. Data were analyzed using Dynamics V7.1.2 software (Wyatt Technology) to calculate hydrodynamic radii (R_h).

Small-angle X-ray scattering

SAXS experiments were conducted at beamline 4-2 at Stanford Synchrotron Radiation Lightsource (SSRL) using a Rayonix MX225-HE detector at a distance of 2500 mm, using 1.13 Å wavelength X-rays. Protein preparations for DLS measurements were used for SAXS data collection. For each protein or complex, scattering intensity was measured at four protein concentrations (0.5–7 mg/mL), collecting 10 exposures of 1 s each, covering a momentum transfer (q) range of 0.0047–0.3751/Å. The scattering profile for the buffer was obtained in the same manner. Scattering curves collected from protein samples were corrected for background scattering using the intensity data collected from the buffer alone using SasTool [31].

SAXS scattering curves were scaled, high and low q regions of scattering curves were merged to extrapolate to infinite dilution, and Guinier analysis was performed using PRIMUS [32]. R_g values were calculated from Guinier plots. Scattering curves were overlaid to check for concentration-dependent effects on the scattering profile. GNOM [17] was used to calculate pairwise distribution functions. Porod volumes were calculated from DATPOROD [33]. Molecular weight was calculated by using the formula $MM_p = I(0)_p/c_p \times (MM_{st})/[I(0)_{st}/c_{st}]$, where MM_p and MM_{st} are molecular masses of the protein and lysozyme standard, respectively; $I(0)_p$ and $I(0)_{st}$ are the scattering angles at zero intensity; and c_p and c_{st} are the concentrations [19]. The protein concentration, c_p, was calculated using the equation $A = \varepsilon L c_p$, where A is absorbance at 280 nm, ε is the molar extinction coefficient, and L is the path length. The extinction coefficient and theoretical molecular weight for a 3:1 and a 1:1 Fab:huntingtin exon 1 protein complex are different. Because we most likely observed a mixture of 1:1, 2:1, and 3:1 Fab:huntingtin complexes, we listed a lower limit (100% 1:1) and an upper limit (100% 3:1) for potential complex sizes.

For each protein or complex, at least 10 *ab initio* models were generated using DAMMIF [34]. Models were superimposed and averaged using DAMMIN [35] and DAMAVER [36] in the ATSAS package [33], and resulting models were filled with dummy atoms.

Supplementary data to this article can be found online at http://dx.doi.org/10.1016/j.jmb.2015.05.023.

Acknowledgements

We thank Beth Huey-Tubman and Alejandra Olvera for technical support; Thomas Weiss, Lester Carter, and the scientific staff of SSRL beamline 4-2 for help with SAXS experiments; Tobias Stuwe for assistance with SEC-MALS experiments; and Beth Stadtmueller and Melanie Brewer for critical reading of the manuscript. We thank R. S. Atwal at the Massachusetts General Hospital for providing the N17 antibody. We acknowledge the Gordon and Betty Moore Foundation for support of the Molecular Observatory at Caltech. The operations at SSRL are supported by the Department of Energy and by the National Institutes of Health. G.E.O. was supported by National Research Service Awards (T32GM7616, 5T32GM008042) from the National Institute of General Medical Sciences and by the Center for Advancement of Science in Space.

Author Contributions: G.E.O. and P.J.B. conceived the study; G.E.O. and D.M.N. performed protein expression, purification, Western and dot blots, and SEC-MALS; G.E.O. performed equilibrium gel-filtration assays; G.E.O., A.P.W., and P.J.B. analyzed the data; and G.E.O. and P.J.B. wrote the paper with all co-authors contributing to scientific planning and discussions.

Received 25 March 2015;
Received in revised form 19 May 2015;
Accepted 20 May 2015
Available online 3 June 2015

Keywords:
equilibrium gel-filtration;
Huntington's disease;
linear lattice;
polyglutamine;
small-angle X-ray scattering

†http://web.expasy.org/protparam/

Abbreviations used:
3D, three-dimensional; DLS, dynamic light scattering; Fab, fragment antigen-binding; HD, Huntington's disease; MALS, multiangle light scattering; polyQ, polyglutamine; SAXS, small-angle X-ray scattering; SEC, size-exclusion chromatography; SSRL, Stanford Synchrotron Radiation Lightsource; TRX, thioredoxin.

References

[1] Zuccato C, Valenza M, Cattaneo E. Molecular mechanisms and potential therapeutical targets in Huntington's disease. Physiol Rev 2010;90:905–81.

[2] Hendricks AE, Latourelle JC, Lunetta KL, Cupples LA, Wheeler V, MacDonald ME, et al. Estimating the probability of de novo HD cases from transmissions of expanded penetrant CAG alleles in the Huntington disease gene from male carriers of high normal alleles (27-35 CAG). Am J Med Genet A 2009;149A:1375–81.

[3] Bennett MJ, Huey-Tubman KE, Herr AB, West AP, Ross SA, Bjorkman PJ. A linear lattice model for polyglutamine in CAG-expansion diseases. Proc Natl Acad Sci USA 2002;99:11634–9.

[4] Li P, Huey-Tubman KE, Gao T, Li X, West AP, Bennett MJ, et al. The structure of a polyQ-anti-polyQ complex reveals binding according to a linear lattice model. Nat Struct Mol Biol 2007;14:381–7.
[5] Trottier Y, Lutz Y, Stevanin G, Imbert G, Devys D, Cancel G, et al. Polyglutamine expansion as a pathological epitope in Huntington's disease and four dominant cerebellar ataxias. Nature 1995;378:4.
[6] Klein FA, Zeder-Lutz G, Cousido-Siah A, Mitschler A, Katz A, Eberling P, et al. Linear and extended: a common polyglutamine conformation recognized by the three antibodies MW1, 1C2 and 3B5H10. Hum Mol Genet 2013;22: 4215–23.
[7] Nagai Y, Inui T, Popiel HA, Fujikake N, Hasegawa K, Urade Y, et al. A toxic monomeric conformer of the polyglutamine protein. Nat Struct Mol Biol 2007;14:332–40.
[8] Miller J, Arrasate M, Brooks E, Libeu CP, Legleiter J, Hatters D, et al. Identifying polyglutamine protein species *in situ* that best predict neurodegeneration. Nat Chem Biol 2011;7: 925–34.
[9] Peters-Libeu C, Miller J, Rutenber E, Newhouse Y, Krishnan P, Cheung K, et al. Disease-associated polyglutamine stretches in monomeric huntingtin adopt a compact structure. J Mol Biol 2012;421:587–600.
[10] Fodale V, Kegulian NC, Verani M, Cariulo C, Azzollini L, Petricca L, et al. Polyglutamine- and temperature-dependent conformational rigidity in mutant huntingtin revealed by immunoassays and circular dichroism spectroscopy. PLoS One 2014;9:e112262.
[11] Cui X, Liang Q, Liang Y, Lu M, Ding Y, Lu B. TR-FRET assays of Huntingtin protein fragments reveal temperature and PolyQ length-dependent conformational changes. Sci Rep 2014;4:5601.
[12] Klein FA, Pastore A, Masino L, Zeder-Lutz G, Nierengarten H, Oulad-Abdelghani M, et al. Pathogenic and non-pathogenic polyglutamine tracts have similar structural properties: towards a length-dependent toxicity gradient. J Mol Biol 2007;371:235–44.
[13] Wyatt PJ. Light scattering and the absolute characterization of macromolecules. Anal Chim Acta 1993;272:40.
[14] Sanchez LM, Penny DM, Bjorkman PJ. Stoichiometry of the interaction between the major histocompatibility complex-related Fc receptor and its Fc ligand. Biochemistry 1999;38:9471–6.
[15] West AP, Giannetti AM, Herr AB, Bennett MJ, Nangiana JS, Pierce JR, et al. Mutational analysis of the transferrin receptor reveals overlapping HFE and transferrin binding sites. J Mol Biol 2001;313:385–97.
[16] Hummel JP, Dreyer WJ. Measurement of protein-binding phenomena by gel filtration. Biochim Biophys Acta 1962;63: 530–2.
[17] Svergun DI. Determination of the regularization parameter in indirect-transform methods using perceptual criteria. J Appl Crystallogr 1992;25:495–503.
[18] Vitalis A, Wang X, Pappu RV. Atomistic simulations of the effects of polyglutamine chain length and solvent quality on conformational equilibria and spontaneous homodimerization. J Mol Biol 2008;384:279–97.
[19] Mylonas E, Svergun DI. Accuracy of molecular mass determination of proteins in solution by small-angle X-ray scattering. J Appl Crystallogr 2007;40:s245–9.
[20] Mertens HD, Svergun DI. Structural characterization of proteins and complexes using small-angle X-ray solution scattering. J Struct Biol 2010;172:128–41.
[21] Rambo RP, Tainer JA. Accurate assessment of mass, models and resolution by small-angle scattering. Nature 2013;496:477–81.
[22] Putnam CD, Hammel M, Hura GL, Tainer JA. X-ray solution scattering (SAXS) combined with crystallography and computation: defining accurate macromolecular structures, conformations and assemblies in solution. Q Rev Biophys 2007; 40:191–285.
[23] Trewhella J, Hendrickson WA, Kleywegt GJ, Sali A, Sato M, Schwede T, et al. Report of the wwPDB Small-Angle Scattering Task Force: data requirements for biomolecular modeling and the PDB. Structure 2013;21:875–81.
[24] Kim MW, Chelliah Y, Kim SW, Otwinowski Z, Bezprozvanny I. Secondary structure of Huntingtin amino-terminal region. Structure 2009;17:1205–12.
[25] Caron NS, Desmond CR, Xia J, Truant R. Polyglutamine domain flexibility mediates the proximity between flanking sequences in huntingtin. Proc Natl Acad Sci USA 2013;110: 14610–5.
[26] Butland SL, Devon RS, Huang Y, Mead CL, Meynert AM, Neal SJ, et al. CAG-encoded polyglutamine length polymorphism in the human genome. BMC Genomics 2007;8: 126.
[27] Schaefer MH, Wanker E, Andrade-Navarro MA. Evolution and function of CAG/polyglutamine repeats in protein–protein interaction networks. Nucleic Acids Res 2012;40:4273–87.
[28] Studier FW. Protein production by auto-induction in high density shaking cultures. Protein Expr Purif 2005;41: 207–34.
[29] Diskin R, Scheid JF, Marcovecchio PM, West AP, Klein F, Gao H, et al. Increasing the potency and breadth of an HIV antibody by using structure-based rational design. Science 2011;334:1289–93.
[30] Atwal RS, Desmond CR, Caron N, Maiuri T, Xia J, Sipione S, et al. Kinase inhibitors modulate huntingtin cell localization and toxicity. Nat Chem Biol 2011;7:453–60.
[31] Smolsky I, Liu P, Niebuhr M, Ito K, Weiss TM, Tsuruta H. Biological small-angle X-ray scattering facility at the Stanford Synchrotron Radiation Laboratory. J Appl Crystallogr 2007;40: 453–8.
[32] Konarev PV, Volkov VV, Sokolava AV, Koch MHJ, Svergun DI. PRIMUS—a Windows-PC based system for small-angle scattering data analysis. J Appl Crystallogr 2003;36: 1277–82.
[33] Petoukhov MV, Franke DS, Shkumatov AV, Tria G, Kikhney AG, Gajda M, et al. New developments in the ATSAS program package for small-angle scattering data analysis. J Appl Crystallogr 2012;45:342–50.
[34] Franke DS, Svergun DI. DAMMIF, a program for rapid *ab-initio* shape determination in small-angle scattering. J Appl Crystallogr 2009;42:342–6.
[35] Svergun DI. Restoring low resolution structure of biological macromolecules from solution scattering using simulated annealing. Biophys J 1999;76:2897-86.
[36] Volkov VV, Svergun DI. Uniqueness of ab-initio shape determination in small-angle scattering. J Appl Crystallogr 2003;36:860–4.
[37] Petoukhov MV, Konarev PV, Kikhney AG, Svergun DI. *ATSAS* 2.1—towards automated and Web-supported small-angle scattering data analysis. J Appl Crystallogr 2007;40:6.